

# Impact of Membrane Types and Catalyst Layers Composition on Performance of Polymer Electrolyte Membrane Fuel Cells

Paritosh Kumar Mohanta,\* Masuma Sultana Ripa, Fabian Regnet, and Ludwig Jörissen<sup>[a]</sup>

Performance of a low temperature polymer electrolyte membrane fuel cell (PEMFC) is highly dependent on the kind of catalysts, catalyst supports, ionomer amount on the catalyst layers (CL), membrane types and operating conditions. In this work, we investigated the influence of membrane types and CL compositions on MEA performance. MEA performance increases under all practically relevant load conditions with reduction of the membrane thickness from 50 to 15  $\mu\text{m}$ , however further decrease in membrane thickness from 15 to 10  $\mu\text{m}$  leads to reduction in cell voltage at high current loads. A thick anode CL is found to be beneficial under wet operating conditions

assuming more pore space is provided to accommodate liquid water, whereas under dry operating conditions, an intermediate thickness of the anode CL is beneficial. When studying the impact of catalyst layer thickness, too thin a catalyst layer again shows reduced performance due to increased ohmic resistance ruled out the performance of the MEAs which have identical Pt crystallite sizes on the cathode CLs i.e. the thinnest the cathode CL, the highest the voltage were achieved at a defined current load. Adaptation of the operating conditions is highly anticipated to achieve the highest MEA performance.

## 1. Introduction


Due to zero emission regulations and high energy conversion efficiency, PEMFC technology is becoming popular to the transport sectors worldwide. However, in order to reduce cost, it is necessary to further increase power density, endurance and simultaneously reduce the noble metal demand. The membrane–electrode assembly (MEA) forms the heart of the PEMFC. Increasing the operating voltage in the practically relevant load conditions is a key factor in further PEMFC development. The MEA is composed of an anode CL, the electrolyte membrane and a cathode CL. Both anode and cathode CL are prepared with catalyst nanoparticles (usually Pt) supported on high surface area carbon black (CB) materials and an ionomer. Electrochemical reactions are taking place where the three phases (ionomer, catalyst and reactant) are in contact. In PEMFC, the oxygen reduction reaction (ORR) kinetics which is taking place in cathode is slower than the hydrogen oxidation reaction kinetics in the anode. By improving the intrinsic catalytic activities of catalysts, enhancement of sluggish ORR kinetics is possible,<sup>[1–4]</sup> resulting in improved MEA performance. In addition, mass transport properties in the catalyst layers are

becoming increasingly important for the performance characteristics of the MEA. Proper design of CLs with optimized pore structure, thickness, ionomer content etc., turned out to be a key factor to improve MEA performance.<sup>[5–16]</sup> Yet, the effects caused by modifications of CL preparation are interacting with each other. The amount of ionomer which is needed for proton transport and to create the triple phase region in both CLs does affect the reactant permeability, the catalytic activity and the ionic resistance simultaneously.<sup>[7]</sup> Permeability of oxygen is found to be increased with decreasing ionomer film thickness in the CL.<sup>[8]</sup> Too thick an ionomer film in the CL, while increasing the proton conductivity, simultaneously causes an increase of reactant diffusion resistance. On the contrary, too low an ionomer content can decrease ionic conductivity and reduce the active triple phase region. Both adversely impact on MEA performance.<sup>[9–10]</sup> Therefore, it is crucial to use the right amount of ionomer in the CL to achieve optimum MEA performance.

Another methodology of improving MEA performance could be the reduction of electronic resistance of each CL. This can be done by reducing thickness of the CL by using catalysts that possess high Pt content, resulting improvement of linear parts of the I-V characteristics of the MEA. However, the CL thickness affects the water management and the reaction to variations of operating conditions.<sup>[14–16]</sup> Proper MEA fabrications and ink formulations can also improve performance characteristics of MEAs.<sup>[13,17–20]</sup>

Types of membrane can change the MEA performance characteristics dramatically.<sup>[21–22]</sup> As a general rule, the thinner the membrane, the lower the ohmic resistance which is leading to higher MEA performance.<sup>[23–24]</sup> Nevertheless, thinner membranes are also leading to increased hydrogen crossover and changes in back diffusion of product water. Both effects are affecting performance and durability's of the MEA.

[a] Dr. P. K. Mohanta, M. S. Ripa, F. Regnet, Dr. L. Jörissen  
Zentrum für Sonnenenergie- und Wasserstoff-Forschung Baden-Württemberg (ZSW)  
Brennstoffzellen Grundlagen (ECG)  
Helmholtzstrasse 8  
89081 Ulm (Germany)  
E-mail: paritosh.mohanta@zsw-bw.de

 © 2020 The Authors. Published by Wiley-VCH Verlag GmbH & Co. KGaA. This is an open access article under the terms of the Creative Commons Attribution Non-Commercial NoDerivs License, which permits use and distribution in any medium, provided the original work is properly cited, the use is non-commercial and no modifications or adaptations are made.

In the present study, the sensitivity of MEA performance on the ionomer content in the CLs, on the membrane types, the thickness of anode CL and cathode CL was investigated step by step. Pt electrocatalysts supported on CB having a noble metal content of 20–50 wt% were prepared via a modified polyol process. The catalysts were then annealed to stabilize the catalyst surface morphologies, which also increases the catalytic activities and the stabilities of the catalysts.<sup>[25–27]</sup>

The catalysts were characterized by measuring Pt crystallite sizes, Pt contents, electrochemical active surface areas (ECSA) and ORR activities. Eventually, catalysts coated membranes were prepared with the catalysts to be investigated to conduct MEA single cell performance tests. A commercial catalyst from the company Tanaka was taken as reference for comparison.

## 2. Results and Discussion

### 2.1. Characterization of Homemade Catalysts

Since Pt crystallite size is affecting the ECSA, a comparative assessment of catalyst and MEA performance needs to take this into account. Table 1 shows the Pt content (via ICP-OES analysis) and the average crystallite sizes of Pt (via XRD) of homemade (annealed) and reference catalysts that were used in this work. As the Pt nanoparticles are closer packed in highly Pt containing catalysts, there is an increased tendency to agglomerate during the annealing process. Thus, the average crystallite size of Pt of the homemade catalysts are slightly increasing with the Pt content from 20 to 50 wt% of the catalysts. Nevertheless, they are still within the limit of < 5 nm, which are usually using as fuel cell catalyst.

Catalyst Name	Pt content / wt% Target	Pt content / wt% actual	Pt crs./ [nm]
CB20	20	17.9	2.2
CB30	30	28.2	2.9
CB35	35	33.3	2.9
CB45	45	43.7	3.3
CB50	50	48.8	4.4
TKV30	30	29.2	1.4
TKV50	50	46.3	1.5

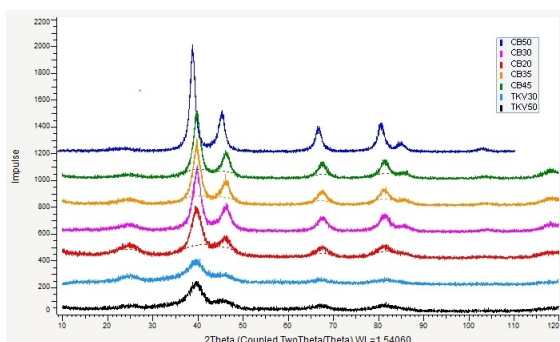


Figure 1. XRD patterns of the catalysts.

XRD patterns (see Figure 1) of the catalysts shows the decreasing of peak broadening from the CB20 to CB50 are due to increasing of Pt crystallite sizes of the catalysts.

In order to get unique performance of each single fuel cell, an even distribution of catalyst-nanoparticles on the support and the CL is required. As a typical example Figure 2 shows TEM images of the CB20 catalyst in which the distribution of Pt particles on CB support is found to be homogeneous. Other catalysts showed similar results.

High ORR active catalyst is required to improve the sluggish cathode kinetics in PEMFC. In order to compare the ORR activities of the catalysts, rotating disk electrode (RDE) measurements using a three electrodes set up in 0.1 M HClO<sub>4</sub> at room temperature (RT) were performed. Table 2 shows the comparison of ORR activities of the homemade and the reference catalysts. The ECSA of the homemade catalysts decreased with increasing the Pt content from 20 to 50 wt% in parallel with the increase of the average Pt crystallite size. As expected, the mass activities of the catalysts were also decreasing accordingly. The reference TKV30 (Tanaka, TEC10V30E, 29.2 wt% Pt on Vulcan XC72) catalyst is showing the highest mass activities compared to the homemade catalysts. Likewise the reference TKV50 (Tanaka, TEC10V50E, 46.3 wt% Pt on Vulcan XC72) also shows low particle size, could be due to the lowest average Pt crystallite sizes, better Pt dispersion, less Pt agglomeration, and larger active surface areas of the TKV30 among others.<sup>[28]</sup>

### 2.2. Impact of Ionomer Content on MEA Performance

The amount of ionomer on the CL has significant impact on MEA performance, since it directly affects proton conduction, reactant diffusion and water management during fuel cell

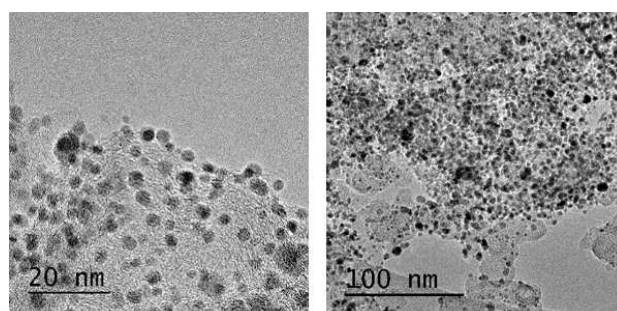


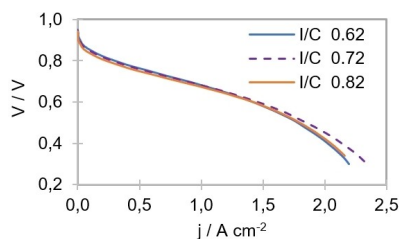
Figure 2. TEM images of CB20 catalyst (17.9 wt% Pt on CB).

Catalyst Name	ECSA/ mg <sup>-1</sup> Pt	MA/ Ag <sup>-1</sup> Pt
CB20	118	580
CB30	102	469
CB35	89	435
CB45	72	167
CB50	67	260
TKV30	113	597
TKV50	57	257

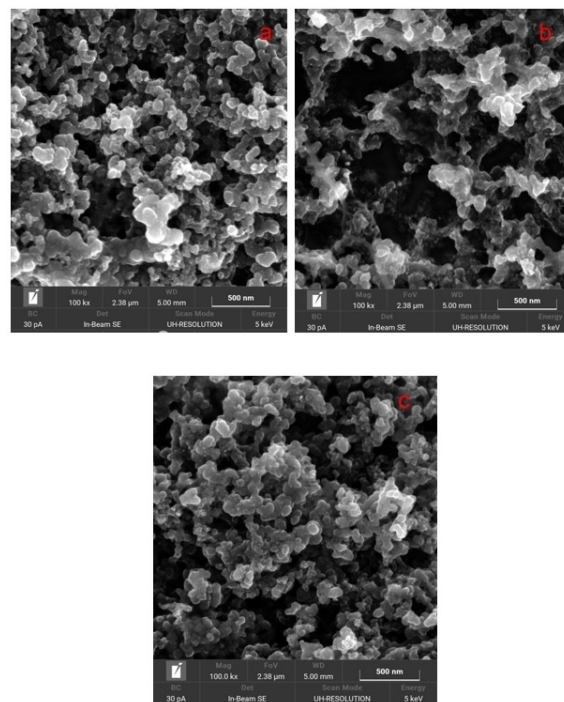
operation. A thin film of ionomer on the catalyst particles is highly desired to reduce the reactant mass transport resistance. However, too little ionomer in the CL can reduce the amount of the so-called triple phase boundaries as well as proton conduction, resulting low MEA performance.<sup>[7–10,29]</sup> A thick layer of ionomer on the CL can increase the protonic conductivity favoring the MEA performance, however, electronic conductivity, reactant diffusivity are decreased causing the MEA performance to decrease. Additionally, it can adversely impact on water management of the cell due to blockage some pores in the CL. Thus, optimization of the ionomer film in each CL is needed to achieve maximum MEA performance. The optimum ionomer content is depending on the Brunauer, Emmett, and Teller (BET) surface areas of the support materials.<sup>[30–33]</sup> Unfortunately, there are no experimental techniques available, except the performance characterization of MEA in a full cell to determine the optimum amount of ionomer needed for each CL. In our previous work an optimum ionomer to carbon ratio (I/C) 0.74 on the cathode CL was found to achieve the highest MEA performance for the catalyst (Tanaka, TEC10E20E) supported on a high BET surface areas CB (800 m<sup>2</sup>g<sup>-1</sup>) material.<sup>[30]</sup> In this work, the optimum ionomer content was investigated for the catalysts supported on Vulcan XC72 having a BET surface area of 192 m<sup>2</sup>g<sup>-1</sup>. Thus, keeping the anode CL constant (TEC10E20E, 19.4 wt% Pt/CB, I/C 0.74), variation of ionomer amount on the cathode CLs were performed. A TKV30 as cathode catalyst and a Nafion™ NR211 (25 μm) membrane were chosen to perform the investigations.

Figure 3 shows the overall MEA characteristics under the same operating conditions while altering I/C between 0.6 and 0.8 on the cathode CL. Among them, the highest voltage at high current loads (> 1 Acm<sup>-2</sup>) were achieved for the MEA prepared with I/C 0.72. We can assume here that the ionomer layer is thick at I/C 0.82 compared to the I/C 0.72. The loss of voltages in the linear part (increase of ohmic resistance) is an explanation here. On the other hand, decreasing of triple phase region as well as protonic conductivities at I/C 0.62 occurred resulting low MEA performance, compared to the MEA prepared with I/C 0.72.

After the MEA performance tests, FIB-SEM images of the cathode CL of each MEA was taken in order to investigate morphologies of the cathode CLs. Figure 4 shows the cathode CL microstructure is interconnected and produced unique pores for the MEA prepared with the I/C 0.72 which managed the



**Figure 3.** Sensitivity of I/C ratio of the catalyst (TKV30) on MEA performances. Operating conditions: end plate 80 °C, Anode and cathode dp (dew point) 80 °C, Anode stoic. 1.3, Cathode stoic. 3.0, at 150 kPa, Nafion211 (25 μm) membrane, Pt loadings 0.1 (anode) and 0.25 (cathode) mg cm<sup>-2</sup>.



**Figure 4.** FIB-SEM images of the cathode CLs of the MEAs with variable I/C (a) 0.62 (b) 0.72 and (c) 0.82-

produced water properly leading to better performance at high current loads compared to the MEA prepared with the I/C 0.82 and 0.62.

### 2.3. Impact of Membrane Types on MEA Performance

Generally, the ionic resistance in the cell is proportional to the thickness of the electrolyte membrane which can dominate the linear part of the I-V characteristic curves. However, reduction of the membrane thickness changes the water management by changing water back diffusion. In this work, the impact of membrane types on MEA performance was investigated by taking membranes with variable thickness from two different manufacturers; Nafion (50 and 25 μm) and GORE-SELECT® (15 and 10 μm). CCMs were prepared from these membranes using a commercial catalyst (Tanaka, TEC10E20E, 19.4 wt% Pt/CB, I/C 0.74) in both, anode and cathode CLs. Characterization of the MEAs were performed by recording the current- voltage curves under otherwise identical operation conditions.

As expected, MEA performances improved upon reduction of the membrane thickness from 50 to 15 μm due to the decrease of overall resistance of the MEAs (see figure 5). Further reduction of MEA thickness from 15 to 10 μm led to a reduction of cell voltage in the high current density region dominated by mass-transport effects.

One of the most commonly used tools of MEA diagnostics for fuel cell research is the electrochemical impedance spectroscopy (EIS). EIS measurements of the MEAs prepared with

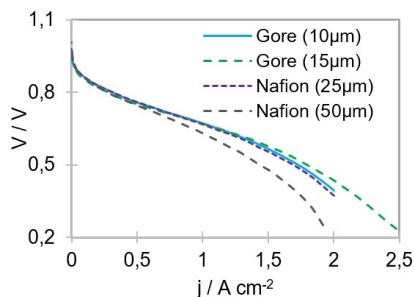


**Figure 5.** Impact of membrane types on I-V curves. Operating conditions: end plate 80 °C, Anode and cathode dp 80 °C, Anode stoic. 1.3, Cathode stoic. 3.0, at 150 kPa, Pt loadings 0.1 (anode) and 0.25 (cathode) mg cm<sup>-2</sup>.

different membranes were performed under the same operating conditions as the performance tests described above.

Figure 6 shows the Nyquist plots at a current load of 1.36 A cm<sup>-2</sup> for all MEAs. As expected, the high frequency resistance decreases with decreasing membrane thickness. However, the diameter of the low frequency arc is decreasing when moving from 50 μm to the 15 μm membrane. Use of the 10 μm membrane leads to a major increase in the low frequency arc diameter indicating that mass transport effects likely caused by water management is playing a major role. MEA prepared with the GORE 15 μm membrane is showing the lowest mass transport losses assuming better water management at 1.36 A cm<sup>-2</sup>. These findings are consistent with the slope of the I-V-curves which are decreasing with decreasing membrane thickness and the curvature of the I-V-curves at high current density. The voltage measured at 1.36 A cm<sup>-2</sup> were 527, 592, 608 and 601 mV from the MEA prepared with Nafion 50, Nafion 25, Gore 15 and Gore 10 membranes also is consistent.

## 2.4. Impact of Anode CL Thickness on MEA Performance

At a given noble metal loading, the thickness of the CL layer is inversely proportional to the Pt-content of the catalyst powder. MEAs prepared from the catalyst with the highest Pt content will result in the thinnest CL resulting in reduction of ohmic and

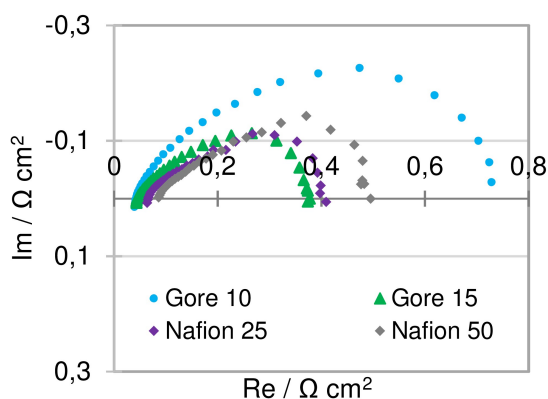


**Figure 6.** Nyquist plots of the MEAs at 1.36 A cm<sup>-2</sup>.

mass-transport resistance. However, manufacturing of ultra-low Pt loaded anode CL is challenging when using a catalyst with high Pt content. Due to the low amount of catalyst spread on the electrode surface, complete catalyst coverage of the electrolyte membrane might not be ensured and in-plane conductivity of the CL might become performance limiting. Furthermore, missing pore volume in the CL may also unfavorably affect water management during operation. To choose a suitable catalyst for the anode CL, a series of MEAs were prepared using commercial Tanaka catalysts supported on Vulcan XC72 containing 20 to 50 wt% Pt (TEC10V20E, TEC10V30E and TEC10V50E) while maintaining the cathode CL (TEC10V50E, 46.3 wt% Pt/CB, I/C 0.72), Pt loadings and membrane unchanged (GORE 15 μm).

I-V characteristics performance of the MEAs at the reference operating conditions shows no significant difference of cell voltages up to 1.6 A cm<sup>-2</sup> current load (see Figure 7 top part), however, at high current loads TKV20 (TEC10V20E, 19.8% Pt/CB) and TKV30 (TEC10V30E, 29.2wt%Pt on CB) showed higher voltage compared to TKV50 (TEC10V50E). On the other hand, when changing the operating conditions from wet (RH 85%) to relatively dry (RH<sub>Anode</sub> 50%, RH<sub>Cathode</sub> 30%) which is closer to the recommended European union reference operating conditions for automotive applications,<sup>[34]</sup> TKV30 showed higher voltages at high current loads ( see Figure 7, lower part).

At our reference operating conditions (RH 85%), a comparatively thick anode CL proved to be beneficial at high current loads. We can assume, cumulated pore volume in the CL prepared with the low Pt content catalyst is higher than the CL prepared with the high Pt content catalysts. At high current loads, water diffusing back from cathode has more chance to distribute in that pore space while still maintaining sufficient

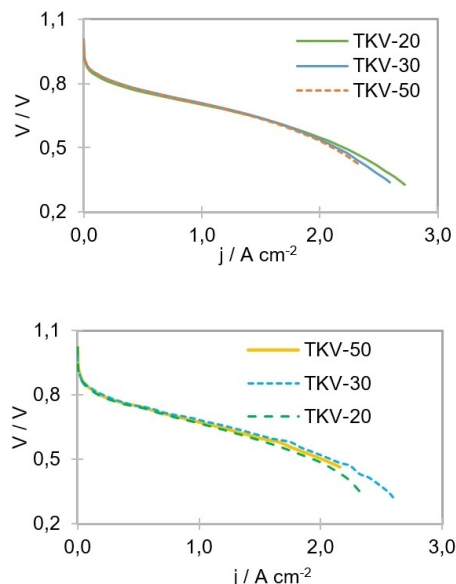


**Figure 7.** I-V characteristics while optimizing anode CL. Operating conditions: end plate 80 °C, Anode stoic. 1.3, Cathode stoic. 3.0, at 150 kPa, Gore membrane (15 μm), Pt loadings 0.1 (anode) and 0.25 (cathode) mg cm<sup>-2</sup>, Anode and cathode dp. 80 °C, (top); Anode and cathode dp. 64 °C and 58 °C respectively (Bottom).

open pore volume for reactant supply. On the other hand, thin anode CL are more likely to suffer from flooding.<sup>[35]</sup> Anode CL made from TKV30 are providing the best compromise between wet and dry operating conditions.

FIB-SEM images shown in Figure 8 are also indicate large volume pore space to accommodate water in operation. Thus, TKV30 was chosen as anode catalyst for comparative studies of homemade catalysts in next steps.

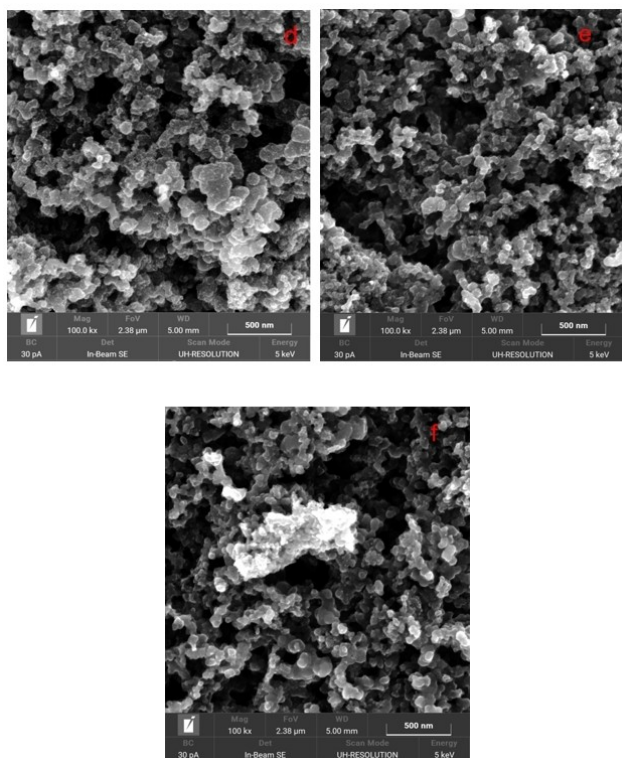


**Figure 8.** FIB-SEM images of the anode CL surfaces of the MEAs prepared with (d) TKV50, (e) TKV30 and (f) TKV20 on the anode CLs.

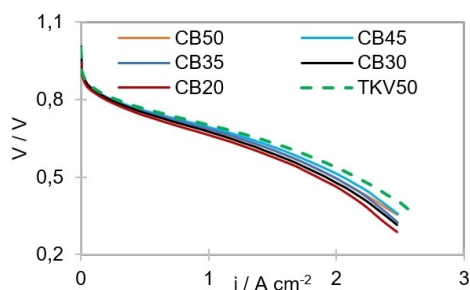


**Figure 9.** I-V characteristics of the homemade and the reference catalysts. Operating conditions: end plate 80 °C, Anode stoic. 1.3, Cathode stoic. 3.0, Anode and cathode dp 80 °C, Anode and cathode inlet 84 °C, at 150 kPa, Gore membrane (15 μm), Pt loadings 0.1 (anode) and 0.25 (cathode) mg cm<sup>-2</sup>.

## 2.5. Impact of Cathode CL Thickness on MEA Performance

In order to investigate the impact of cathode CL thickness on MEA performance, cathode CL of constant noble metal loading were prepared using catalysts with different noble metal content. Thus 20 to 50 wt% Pt containing homemade and a TKV50 (reference) catalysts were used to prepare cathode CL, resulting decreasing of cathode CL thickness with increasing Pt content of the catalysts. Membrane types (Gore 15 μm), anode CL (TKV30, 0.72 I/C), Pt loadings on each CL (0.1 and 0.25 mg cm<sup>-2</sup> in anode and cathode side respectively) and operating conditions were kept constant throughout this investigation.

Figure 9 displays that except CB50, cell voltages are decreasing with increasing thickness of the cathode CL up to about 2 A cm<sup>-2</sup> current load, due to increase of ohmic resistance of the CLs. However, the behavior at high current loads was influenced by different phenomena which may be linked to CL microstructures, water managements, I/C ratio, catalysts particle sizes and intrinsic properties of the catalysts. Lower MEA performance of CB50 than CB45 and CB35 could be due to the limitation of reactive catalyst sites caused by the larger particle diameter (lower ECSA) became dominating. As the average crystallite size of Pt of the reference catalyst (TKV50) is the smallest, and the thinnest CL can be produced by the use of that catalyst, the highest MEA performance of the reference catalyst than that of homemade catalysts was expected.<sup>[36]</sup> However, among all of the homemade catalysts, MEAs prepared with CB45 showed comparable performances as the reference TKV50. For example, at 1 and 1.6 A cm<sup>-2</sup> current loads, it showed 9 and 18 mV lower cell voltages than the reference catalyst respectively (see Table 3).

I-V characteristics of the homemade 20 to 45 wt% Pt containing catalysts showed that ohmic resistances are the dominating factor for the linear parts of the MEA performance curves since they possess identical crystallite sizes of Pt, the thinnest the CL (high Pt containing catalyst), the highest the voltage at a defined current load was observed (see Table 1 and Table 3).

Typically, at high current loads mass transport is highly dominated by water management of the CLs. Thus, the sensitivity of reactants relative humidity of the MEA prepared with homemade (CB45) and the reference catalysts were additionally studied. A series of measurements were performed by changing the relative humidity (dew point temperatures) in

**Table 3.** Dependency of catalyst layers thickness on cell voltages of the MEAs at defined current load extracted from the figure 6.

MEA	Cell Voltage/V				
	OCV	0.016 A	1.04 A	1.6 A	2 A
TKV50	1.009	0.899	0.697	0.617	0.538
CB20	0.940	0.880	0.656	0.558	0.463
CB30	1.004	0.894	0.669	0.571	0.477
CB35	0.987	0.887	0.692	0.587	0.495
CB45	1.003	0.895	0.688	0.599	0.513
CB50	0.972	0.890	0.676	0.585	0.495

\*cell voltage [V] at defined current loads.

both anode and cathode while keeping other operating parameter unchanged. It has been found that relatively wet anode (68% RH, dp75 °C) and dry cathode (45% RH, dp 65 °C) could raise the voltage in the mass transport region significantly compared to the reference operating conditions (85% RH, dp 80 °C). Figure 10 shows this influence of operating conditions. Solid lines are representing the reference operating conditions and the dotted lines are the adapted operating conditions.

A transparent view of dependency of RH on MEA performances can be seen from the figure 11 (extracted from figure 10) at defined current loads. Both homemade and the reference catalysts are showing the same responses when the cell operating conditions are changed from wet to dry. Firstly, the open circuit voltages (OCV) are increasing then slightly decreasing the voltages up to approximately 0.8 A cm<sup>-2</sup> current load may be due to the increase of membrane resistance and/or ionomer resistance on the CLs, since they are comparatively dry and the product water is not sufficient to compensate the water uptake in the gas flow leaving the cell. Further increase of load currents are favorable as more water is produced which is needed for the membrane humidification. Due to the low cathode RH, no water condensation was expected. As a result, we assume higher free pore volume, lower reactant transport losses, and subsequently higher voltages.

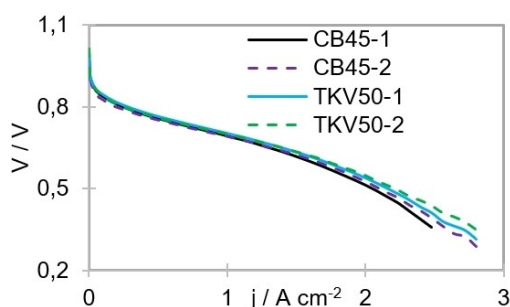


**Figure 10.** I-V characteristics of the homemade and the reference catalysts. Operating conditions: end plate 80 °C, Anode stoic 1.3, Cathode stoich 3.0, Anode and cathode inlet 84 °C, at 150 kPa, Gore membrane (15 μm), Pt loadings 0.1 (anode) and 0.25 (cathode) mg cm<sup>-2</sup> (a) solid lines : Anode and cathode dp 80 °C (b) Anode and cathode dp 75 °C and 65 °C respectively.

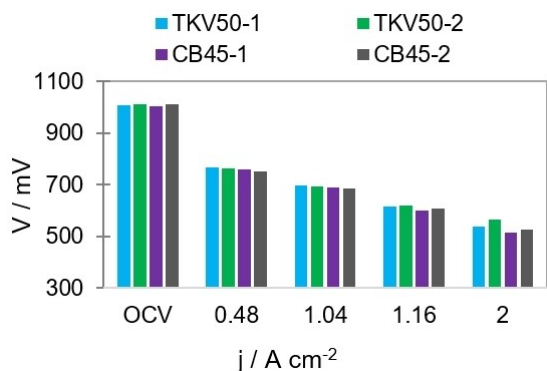


**Figure 11.** Comparison of I-V characteristics of the homemade and the reference catalysts at defined current load under wet and dry operating conditions (extracted from Figure 10).

Likewise other MEAs, FIB-SEM images of the MEAs prepared with the reference (TKV50) and the best homemade catalysts (CB45) were done (see Figure 12). No significant morphological differences were observed in cathode CL images of these MEAs. Thus, we can assume, the small performance differences between TKV50 and CB45 were caused by the lower Pt-crystallite size as well as the lower cathode CL-thickness of the MEA prepared with TKV50 compared to the homemade catalyst CB45.

In addition to variation of humidity, we also investigated the impact of pressure and stoichiometry on the MEA performance. As expected, we found a significant impact of pressure and cathode stoichiometry on MEA performance (see table 4 and Figure 13).

Figure 13 shows the influence of MEA performance at three different i.e. reference (TKV50-1), relatively dry (TKV50-2) and advance (TKV50-3) operating conditions (see Table 4). Due to improvement of water management and reactant utilization (at high pressure) additional enhancement of MEA performance at high current load was attained, for example at 2 A cm<sup>-2</sup> current

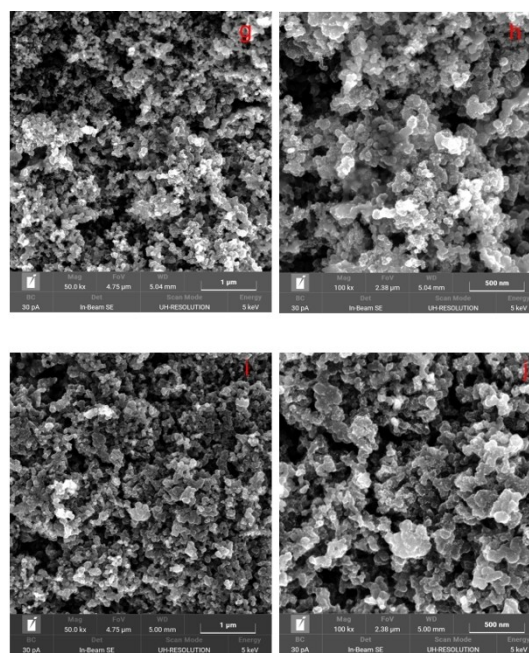


**Figure 12.** FIB-SEM images of the cathode CL surfaces of the MEAs prepared with CB45 (g and h) and TKV50 (i and j) catalysts at two different magnifications.

**Table 4.** MEA operating conditions.

Parameters	Reference (TKV50-1)	Dry (TKV50-2)	Advance (TKV50-3)
Cell Temperature	80 °C	80 °C	80 °C
Inlet Temperature	84 °C	84 °C	84 °C
Dew point Anode	80 °C	75 °C	75 °C
Dew point cathode	80 °C	65 °C	65 °C
Anode Stoic.	1.3	1.3	1.3
Cathode Stoic.	3.0	3.0	4
Anode inlet	150 kPa	150 kPa	200 kPa
Cathode inlet	150 kPa	150 kPa	180 kPa

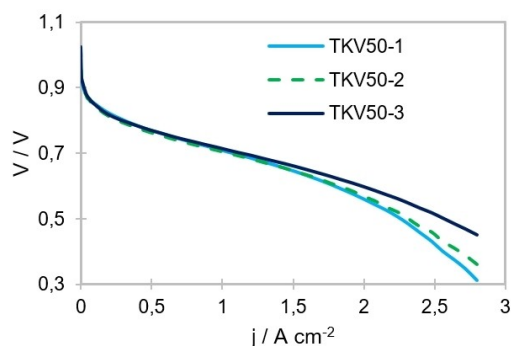


**Figure 13.** I-V characteristics of TKV50 at three different operating conditions (see Table 4). Gore membrane (15  $\mu\text{m}$ ), Pt loadings 0.1 (anode) and 0.25 (cathode)  $\text{mg cm}^{-2}$ .

load, 560, 569 and 598 mV voltages were measured from the three different operating conditions respectively.

### 3. Conclusion

Proper understanding of each component effects on MEA performance is necessary to increase the power density of a PEMFC under high current load conditions. Starting from the catalyst nanostructure, we developed a robust synthesis process of 20 to 50 wt% Pt containing catalysts supported on CB. Although after annealing the average Pt particle sizes in the catalysts increased, they were still between 2.2 nm (CB20) and 4.4 nm (CB50) that are usually needed for PEMFC applications.

Next, the influence of membrane types, ionomer content (I/C) on the CLs, anode catalysts (20 to 50 wt% Pt), and eventually cathode catalysts (20 to 50 wt% Pt) and operating conditions on MEA performances were investigated.

MEA performance are highly sensitive to I/C ratio in the CL. The optimum I/C ratio is mainly depending on the types of support materials, particularly the BET surface areas of the support materials. An I/C ratio of 0.72 was found to be optimum for CB supported catalysts in the present reference cell operating conditions.

MEA performances were found to be the highest upon reduction of membrane thickness from 50 to 15  $\mu\text{m}$  due to the decrease of ohmic resistance of the MEAs. Further reduction of MEA thickness from 15 to 10  $\mu\text{m}$  turned out unfavorable, despite decreasing high frequency resistance, additional mass transport effects are becoming evident in the I-V characteristic performance as well as in EIS measurements thus lowering the cell voltage under high current load.

At our reference operating conditions, a thick anode CL is favorable at high current loads assuming back diffused water from the cathode distributes in open pores of the anode CL, indirectly improving the water management on the cathode side as well. However, under dry operating conditions thin or intermediate thickness of the anode CL is found to be advantageous since no condensate in the CL is restricting reactant transport.

Mass activities as well as ECSA of the homemade catalysts were found lower than the industrial reference catalysts; however, the MEAs prepared with the homemade catalysts showed comparable performance and mass transport behavior when investigated in single cell tests.

Ohmic resistances are governing the performance of the MEA prepared with homemade 20 to 45 wt% Pt containing catalysts which have identical Pt crystallite sizes. The thinner the cathode CL (CB45), the higher the voltage were achieved at a defined current load.

In order to achieve the maximum performance of a MEA, one should select an optimum anode and cathode CL thickness and adapted ionomer to carbon ratio in either of the CLs. Apparently, the catalyst layer must enable high rates of reactant transport to the reaction site as well as product water removal. We assume that too thin a catalyst layer can become flooded in operation under high RH. It is likely that adaptation of the operating conditions (humidification, stoichiometry, temperature and pressure) to the electric load can mitigate the effects observed. This will be subject of further investigations.

### Experimental Section

A Vulcan XC72 (Cabot) was taken as support for preparing 20 to 50 wt% Pt containing catalysts. The synthesis procedure was almost identical to the process described in our previous work,<sup>[30]</sup> except a variation of the pH value which was adjusted between 11 and 12 with 1 M NaOH solution (in 50 vol% ethylene glycol in water) during synthesis of Pt nanoparticles. In brief, to get 5 g of 30 wt% Pt electro catalyst, 3.5 g of CB support material was suspended in 150 ml ultrapure water in a 1 L three neck round bottom flask. The mixture was then stirred for 2 minutes followed by sonicated in an ultrasonic bath for 10 minutes. After sonication, the mixture was placed in an electric heater which was placed on a magnetic stirrer plate for constant stirring. 150 ml of Ethylene Glycol (EG, Sigma Aldrich) was then added to the suspension. A gentle flow of Argon gas was continuously allowed to pass through the flask until end of the synthesis process to remove gaseous reaction products. 37.5 mL of Pt stock solution (106.2 g of Chloroplatinic acid hexahydrate from Alfa Aesar in 1 L of ultrapure water) was then added drop wise to the mixture. After that, the required volume of ultrapure water and EG were added to the mixture to adjust the total volume to 500–550 ml in which the ratio of water and EG was exactly 1:1. Finally, pH of the solution was increased from around 1.5 to 11 by adding 1 M NaOH solution (1:1 water and EG) dropwise. The system was then thermally insulated to avoid excessive heat loss and was heated to reach 120 °C by using an electric heater. When the temperature of the mixture was reached to 120 °C, the electric heater's set value was readjusted to maintain 120 °C (mixture temperature) for 1 hour to complete the reduction process. After that, the mixture was kept openly to cool down to 40–50 °C and then filtered by using a vacuum pump. The residue was washed with hot ultrapure water several times till the filtrate is free from Chloride ions. Finally, the residue was dried in an air oven at 70 °C for overnight. Annealing of the dried catalysts were then performed at 250 °C for 1 hour in reducing environment (95 vol% Ar and 5 vol% H<sub>2</sub>) in order to increase the ORR activities and the stabilities of the catalysts.

A Spectra Acros (Acros FHS12) inductively coupled plasma optical emission spectrometry (ICP-OES) instrument was used to measure the actual Pt content in the prepared catalysts.

The average particle sizes of Pt were determined with a Siemens D5000 XRD instrument using the TOPAS software (Bruker AXS, Version 5). Transmission electron microscopic (TEM) images of the prepared catalysts were also performed to observe the distribution of Pt particles in the catalyst powders.

ORR activities of the catalysts were performed using a Pine potentiostat and a Gamry instrument (RDE710) setup in 0.1 M HClO<sub>4</sub> electrolyte at RT. The experimental setup and procedures were very similar as described in references.<sup>[37–38]</sup> In brief, 2.5 to 5 mg of each catalyst (depends on Pt content of the catalyst) was suspended in 5 mL of solvent (0.02 wt% ionomer in 50 vol% IPA in water, pH 9) and was stirred for 1 h. The mixture was then sonicated in an ultrasonic bath for 15 minutes prior to pipetting. 7  $\mu$ L of the suspension (2  $\mu$ g Pt loading) was then taken from the mixture using a micropipette (Corning Lambda plus) and was placed on a gold rotating disk electrode (5 mm outer diameter) followed by drying at 20 RPM by inverting the rotating shaft of the RDE. A Hg/Hg<sub>2</sub>SO<sub>4</sub> (ALS Co. Ltd) and a Pt wire were used as reference and counter electrodes respectively. 120 mL of 0.1 M HClO<sub>4</sub> solution was taken in an electrochemical cell (gamry) and then a gentle flow of N<sub>2</sub> gas was bubbled through the electrolyte for 15 minutes to make the electrolyte O<sub>2</sub> free. The working electrode potential was swept between 0.05 and 1.2 V vs reversible hydrogen electrode (RHE) at 150 mVs<sup>-1</sup> scan rate until getting reproducible CVs. Subsequently, five CVs were recorded within the same potential ranges at 50 mVs<sup>-1</sup> in order to correct background current and to determine electrochemical active surface areas (ECSA) of the catalysts. After that, O<sub>2</sub> saturation of the electrolyte was performed by flowing 0.4 L min<sup>-1</sup> O<sub>2</sub> gas through the electrolyte for 40 minutes. CVs were then taken between 0.05 and 1.2 V vs RHE at 50 mVs<sup>-1</sup> scan rate at 200, 400, 700, 900 and 1600 RPM. IR compensation was done for each measurement automatically via the software. Mass activities of the catalysts at 0.9 V vs RHE were then calculated from the measured data using a koutecky-levich plot.<sup>[39]</sup>

Catalyst coated membranes (CCM) were prepared by manual spray-coating technique using an airbrush. MEA preparation and testing protocols were already described elsewhere.<sup>[31]</sup> Nafion® NR-212 (50  $\mu$ m), Nafion® NR-211 (25  $\mu$ m), GORE SELECT (15  $\mu$ m) and GORE SELECT (10  $\mu$ m) types membranes were used to prepare MEAs. Anode and cathode Pt loadings were set 0.1 mg cm<sup>-2</sup> and 0.25 mg cm<sup>-2</sup> respectively.

Prior to prepare of CCMs, Nafion and GORE (10  $\mu$ m) membranes were conditioned stepwise by heating them at 90 °C for 1 h in each solvent; 3% H<sub>2</sub>O<sub>2</sub>, 0.5 M H<sub>2</sub>SO<sub>4</sub> and ultrapure water. On the other hand, Gore (15  $\mu$ m) membrane was used as received condition. Gore (15  $\mu$ m) membrane has two specific sides, coated blackish side was always used as cathode throughout this work (recommended by the manufacturer).

After spray coating, MEAs were hot pressed at 140 °C at 100 bar for 4 minutes then sandwiched between two gas diffusion layers (SGL, BC29) in a Fuel Cell Technology (FCT) single cell housing of 25 cm<sup>2</sup> (5 cm \* 5 cm) active surface areas and a triple serpentine flow fields. The cell was assembled in a greenlight innovation test station (G20) to conduct the I-V characteristic performances of the MEAs. Pure hydrogen and air were used as fuels. Otherwise mentioned, the cells were operated at 80 °C, anode and cathode stoichiometry 1.3 and 3.0 respectively, 150 kPa pressure, anode and cathode dew point temperatures 80 °C, and anode and cathode inlet temperatures 84 °C.

Initially, break-in of all MEAs were done by applying a square type load cycling between 12 and 16 A (10 minutes holding times of each point) in a repeating manner for five hours. Polarization curve

is obtained by applying the load from the maximum load to the no load currents (descending) and from the no load to the maximum load currents (ascending). After the test, data was evaluated by taking the average cell voltage from the last 30 seconds measurement data of each load point with using a Microsoft chart tools software. I-V curve was then plotted by taking average value of descending and ascending load currents and voltages.

EIS of the MEAs were performed just after completion of the single cell performance test. A Zahner P241 potentiostat in combination with the Greenlight Innovation test bench were used to conduct the tests.

Finally, CLs morphologies were investigated by taking images with a FIB-SEM (Tescan S9000) instrument.

## Acknowledgements

Authors are highly acknowledged to Federal Ministry of Transport and Digital Infrastructure (BMVI), Germany for funding of the project ASI (03B10103A1/03B10103A2). Authors are also grateful to Dr. Rongji Liu and Prof. Carsten Streb, Institute of Inorganic Chemistry 1, Ulm University to perform the TEM measurements.

## Conflict of Interest

The authors declare no conflict of interest.

**Keywords:** PEFMC · fuel cells · MEA · Pt catalysts · ORR catalysts

- [1] I. E. L. Stephens, A. S. Bondarenko, U. Grønberg, J. Rossmeisl, I. Chorkendorff, *Energy Environ. Sci.* **2012**, *5*, 6744.
- [2] Y. Wang, W. Long, L. Wang, R. Yuan, A. Ignaszak, B. Fang, D. P. Wilkinson, *Energy Environ. Sci.* **2018**, *11*, 258.
- [3] V. R. Stamenkovic, B. Fowler, B. S. Mun, G. F. Wang, P. N. Ross, C. A. Lucas, N. M. Markovic, *Science* **2007**, *315*, 493.
- [4] L. Dubau, T. Asset, R. Chattot, C. Bonnaud, V. Vanpeene, J. Nelayah, F. Maillard, *ACS Catal.* **2015**, *5*, 5333.
- [5] S. Litster, G. McLean, *J. Power Sources* **2004**, *130*, 61.
- [6] Shen P. (2008) PEM Fuel Cell Catalyst Layers and MEAs. In: Zhang J. (eds) PEM Fuel Cell Electrocatalysts and Catalyst Layers. Springer, London.
- [7] G. Sasikumar, J. W. Ihm, H. Ryu, *J. Power Sources* **2004**, *132*, 11.
- [8] D. Chen, A. Kongkanand, J. Jorne, *J. Electrochem. Soc.* **2019**, *166*, F24.
- [9] A. Kongkanand, M. F. Mathias, *J. Phys. Chem. Lett.* **2016**, *7*, 1127.
- [10] A. Orfanidi, P. Madkikar, H. A. El-Sayed, G. S. Harzer, T. Kratky, and H. A. Gasteiger, *J. Electrochem. Soc.* **2017**, *164*, F418.
- [11] B. Chi, S. Hou, G. Liu, Y. Deng, J. Zeng, H. Song, S. Liao, J. Ren, *Electrochim. Acta* **2018**, *277*, 110.
- [12] S. Shahgaldi, I. Alaefour, X. Li, *Appl. Energy* **2018**, *217*, 295.
- [13] G. Doo, J. H. Lee, S. Yuk, S. Choi, D. H. Lee, D. W. Lee, H. Kim, S. Kwon, S. G. Lee, H. T. Kim, *ACS Appl. Mater. Interfaces* **2018**, *10*, 17835.
- [14] I. V. Zenyuk, P. K. Das and A. Z. Weber, *J. Electrochem. Soc.* **2016**, *163*, 7, F691.
- [15] M. B. Sassin, Y. Garsany, R. W. Atkinson III, R. M. E. Hjelm, K. E. Swider-Lyons, *Int. J. Hydrogen Energy* **2019**, *44*, 16944.
- [16] T. Soboleva, K. Malek, Z. Xie, T. Navessin, S. Holdcroft, *ACS Appl. Mater. Interfaces* **2011**, *3*, 6, 1827.
- [17] S. J. Shin, J. K. Lee, H. Y. Ha, S. A. Hong, H. S. Chun, I. H. Oh, *J. Power Sources* **2002**, *106*, 146.
- [18] T. H. Yang, Y. G. Yoon, G. Park, W. Lee, C. S. Kim, *J. Power Sources* **2004**, *127*, 230.
- [19] W. Wang, S. Chen, J. Li, W. Wang, *Int. J. Hydrogen Energy* **2015**, *40*, 4649.
- [20] M. Chisaka, H. Daiguji, *Electrochim. Acta* **2006**, *51*, 4828.



- [21] S. Shimpalee, V. Lilavivat, H. Xu, J. R. Rowlett, C. Mittelsteadt, J. W. Van Zee, *J. Electrochem. Soc.* **2018**, *165*, 1019.
- [22] S. Kim, I. Hong, *J. Ind. Eng. Chem.* **2010**, *16*, 901.
- [23] A. Bayrakçeken, S. Erkan, L. Türker, İ. Eroğlu, *Int. J. Hydrogen Energy* **2008**, *33*, 165.
- [24] R. B. Ferreira, D. S. Falcão, V. B. Oliveira, A. M. F. R. Pinto, *Electrochim. Acta* **2017**, *224*, 337.
- [25] C. W. B. Bezerra, L. Zhang, H. Liu, K. Lee, E. P. Marques, A. L. B. Marques, H. Wang, J. Zhang, *J. Power Sources* **2007**, *173*, 891.
- [26] K. Han, Y. Moon, O. Han, K. Hwang, I. Kim, H. Kim, *Electrochem. Commun.* **2007**, *9*, 317.
- [27] N. V. Long, C. M. Thi, N. Masayuki, O. Michitaka, September 26, **2012**. Available from: <https://www.intechopen.com/books/heat-treatment-conventional-and-novel-applications/novel-pt-and-pd-based-core-shell-catalysts-with-critical-new-issues-of-heat-treatment-stability-and->
- [28] S. Shahgaldi, J. Zhao, I. Alaefer, X. Li, *Fuel* **2017**, *208*, 321.
- [29] A. Suzuki, U. Sen, T. Hattori, R. Miura, R. Nagumo, H. Tsuboi, N. Hatakeyama, A. Endou, H. Takaba, M. C. Williams, A. Miyamoto, *Int. J. Hydrogen Energy* **2011**, *36*, 2221.
- [30] P. K. Mohanta, C. Glökler, A. O. Arenas, L. Jörissen, *Int. J. Hydrogen Energy* **2017**, *42*, 27950.
- [31] P. K. Mohanta, Ph.D. Thesis, Ulm Universität, Ulm, Germany, **2017**.
- [32] P. K. Mohanta, F. Regnet, L. Jörissen, *Materials* **2018**, *11*, 907.
- [33] P. K. Mohanta, F. Regnet, L. Jörissen, *Energy Technol.* **2020**, 2000081.
- [34] G. Tsotridis, A. Pilenga, G. D. Marco, T. Malkow, EU harmonised test protocols for PEMFC MEA testing in single cell configuration for automotive applications, EU publications **2016**.
- [35] Y.-H. Cho, H.-S. Park, Y.-H. Cho, D.-S. Jung, H.-Y. Park, Y.-E. Sung, *J. Power Sources* **2007**, *172*, 89.
- [36] E. Carcadea, M. Varlam, A. Marinou, M. Raceanu, M. S. Ismail, D. B. Ingham, *J. Hydrogen Energy* **2019**, *44*, 12829.
- [37] T. J. Schmidt, H. A. Gasteiger, G. D. Stäb, P. M. Urbar, D. M. Kolb, R. J. Behm, *J. Electrochem. Soc.* **1998**, *145*, 2354.
- [38] T. Ikuma, S. S. Kocha, *J. Power Sources* **2010**, *195*, 6312.
- [39] New Energy and Industrial Technology Development Organization (NEDO), PEFC Evaluation Project, Cell Evaluation and Analysis Protocol Guideline (Electrocatalysts, Supports, Membrane, and MEA), Daido University, Ritsumeikan University, Tokyo Institute of Technology, Japan Automobile Research Institute **2014**.

---

Manuscript received: April 1, 2020

Revised manuscript received: April 30, 2020